Elsharkawy *et al.*
Journal of Electrical Systems and Inf Technol (2022) 9:19
https://doi.org/10.1186/s43067-022-00061-2

Journal of Electrical Systems and Information Technology

RESEARCH Open Access

The effect of nonlinear loads on the underground distribution cables: a case study

Tamer M. Z. Elsharkawy*, Gomaa F. A. Osman and Waleed A. A. Salem

*Correspondence:
tamer.elsharkawy@bhit.bu.edu.eg

Department of Electrical Engineering, Benha Faculty of Engineering, Benha University, Banha, Egypt

Abstract

Nonlinear loads have become more prevalent in all applications, including computers, transformers, and adjustable speed drives. The harmonic level of the underground distribution cables rises as a result of these loads. As a result, the cable layers' temperatures are affected by the harmonic levels. The purpose of this paper is to calculate the temperature distribution of a cable conductor and the soil around it under cyclic loading conditions, including the impact of linear and nonlinear loads. The IEC 60,853-2 standard is used to consider the thermal model of an underground cable. The finite element method is investigated to obtain a heat map of the cable layers and their surrounding soil. In this study, the small-scale model was constructed in the laboratory. The cable is installed using two methods at the same loading conditions. The heat transfer in the four-core low-voltage cable installation is measured. Furthermore, total harmonic distortion is measured using a Fluke 125 scope meter. The experimental results from the laboratory model proved that there was an extreme increase in the temperature of cable layers when the cable was installed inside the polyvinyl chloride duct in the soil compared with its installation directly buried in the soil. The results of the experimental tests are compared with simulation results.

Introduction

The generated heat from the cable conductor to the surrounding soil plays a vital role in the performance of the underground distribution cables. The current carrying capacity (ampacity) of underground cables is based on the properties of cable construction and the physical characteristics of the surrounding soil according to the specifications of standard IEC 60,287-1-3 [1]. Moreover, harmonic currents in underground distribution cables can cause unacceptable problems, including overheating of cable layers. The main sources of harmonic currents are the nonlinear loads used in distribution system networks [2, 3]. These result in a gradually higher level of harmonic currents [4, 5]. These harmonic current frequencies cause thermal aging of the cable and increase the strain on the cable insulation [6]. Experimental studies and mathematical simulations of temperature dissipation in underground power cable parts were presented in [7, 8]. The thermal resistance of a soil layer model with very dry soil around the cable was studied in [9, 10]. The authors reported on the thermal analysis of underground cables using

multicore or single cables directly buried or in ducts using the two-dimensional finite element method (FEM), as well as the effect of soil thermal conductivity, in [11–14]. Many studies have discussed the effects of non-sinusoidal currents on the parameters of parallel cables with consideration of the AC resistance, proximity, skin effect, and eddy currents [15, 16]. Furthermore, [17, 18] investigated the power loss simulation in low-voltage cables due to non-sinusoidal loads. A method used in calculating the effect of ampacity on concentric neutral cables due to unbalanced currents and harmonics includes temperature of the cable parts in [19]. The effects of harmonics on the underground power cable were performed, taking into account harmonics measurement [20, 21]. The equation of Neher and Mc Grath was similar to the calculation of the cable ampacity by IEC60287 [22] and was not suitable for unbalance loading cases. The heat transfer effect of pipes and sand on the temperature distributions of the underground cables was presented in [23].

The thermal behavior of buried medium-voltage underground cables in different depths and soil resistivity values under high load operating conditions were presented in [24]. Gouda [25] describes the effects of harmonic orders on cable ampacity and thermal resistance of the soil around the cable. Unfortunately, little of the research does experiment with the heat transfer of underground distribution cable, which is installed in a PVC duct in the presence of harmonic currents under dynamic loading conditions. This paper presents the effect of harmonic current orders on the temperature of the underground distribution cable layers and their surrounding medium. Two installation methods of the low-voltage underground distribution cable are being studied. It is installed inside the PVC duct in the soil and directly buried in the soil. Experimental work and thermal analysis are done in this paper. The calculations of the cable layer temperatures are performed on both sinusoidal and non-sinusoidal loads. It is noticed that there is a serious increase in the temperature of the cable layers in PVC installation in the presence of harmonic currents. These increase due to storing the generated heat in the PVC duct while there is no remarkable rise in the soil temperature.

Finally, this paper presented a comparison between two installation methods on the temperature of underground distribution cable layers and their surrounding soil in the presence of harmonics with THD = 50.8% under dynamic loading conditions. The temperatures are measured by thermocouples. The results of experimental tests, thermoelectric equivalent method (TTE), and finite element method (FEM) are very close.

Experimental system

An experimental study investigated different sources of linear and nonlinear loads that can be used as dynamic loads. The study was performed on the four-core low-voltage underground distribution cable with an aluminum conductor. The cable is installed with two methods: directly buried in the soil and installed in the PVC duct. Figure 1 shows the block diagram of the proposed laboratory system. Figure 2 shows the overall experimental testing system. This system consists of an isolated wooden box simulating an area of the soil surface surrounding the tested cable. The frame of a wooden box consists of two sections of wood with thermal insulation. The cable is buried at a distance of 25 cm from the bottom of the wooden box and 60 cm from the surface of the soil. The required current to test cable is produced by linear loads such as resistive banks and

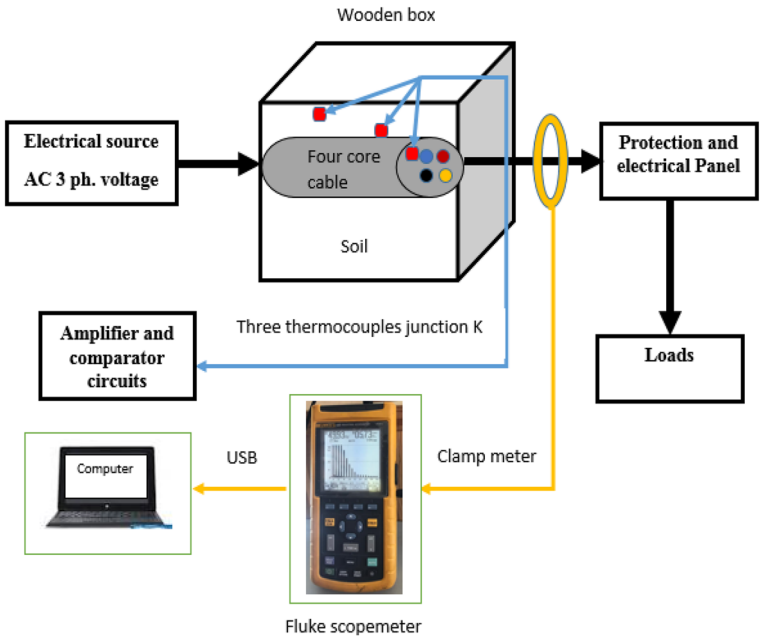

Fig. 1 Block diagram of experimental system

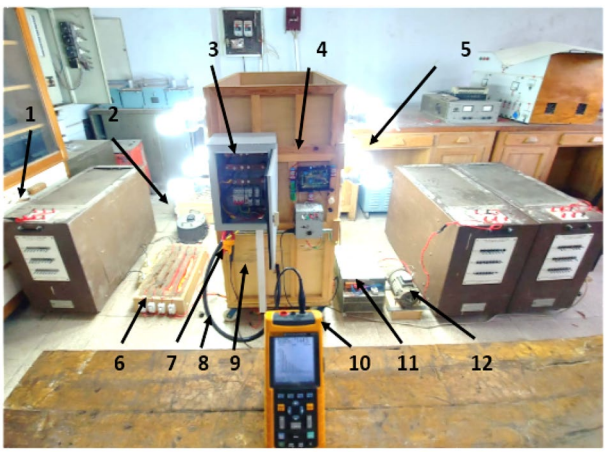

1-Resistive bank	5- Florescent lamps	9-Isolated wooden box
2-Auto-transformer	6- Tungsten coil	10- fluke 125
3- Protection and electrical panel	7- Clamp meter	11-Variable drive
4- Amplifier and comparator circuits	8- Cable under test	12- DC motor

Fig. 2 Overall experimental testing system

tungsten coils. In addition, there are nonlinear loads such as compact florescent lamps, an adjustable variable speed drive connected to a DC motor, and an auto-transformer, which is a source of harmonics in the system. The Fluke 125 scope meter is used to read the current following in each phase. Fluke view software allows us to read the current harmonic orders from the scope meter into a window on the computer screen using the

Fig. 3 Lower section of an isolated wooden box

Table 1 Cable characteristics

Characteristic	Value	Unit
Long of cable used	1	m
Cross-section area of an aluminum conductor	16	mm^2
Nominal thickness of insulation	0.7	mm
Nominal thickness of outer PVC sheath	1.8	mm
Overall diameter of cable	19	mm
Permissible operating temperature	90	°C
Thermal resistivity of the soil	0.968	°C m/W
Current carrying capacity in the ground	68	A
Current carrying capacity in the duct	52	A

optically isolated USB cable OC4USB or the optically isolated RS-232 cable PM9080. Also, it shows the harmonic orders as a percentage of fundamental current and the percentage of total harmonic distortion (THD) in each phase. The temperature of the cable layers and their surrounding soil is read by a thermocouple junction (K) with a temperature range of 0 to 200 °C and accuracy ± 2.2 °C% or ± 0.75%. An amplifier and a comparator circuit are connected to the output of the thermocouple junction (K) to amplify the output of the thermocouple. The output of the control circuit is connected to the monitoring device.

Experimental setup

The installation methods are tested inside a laboratory in an isolated wooden box to simulate an area of the soil surface surrounding the tested cable. The wooden box consists of two identical sections measuring 50 cm wide, 100 cm long, and 50 cm high. Its frame consists of two sections of wood with thermal insulation of 2.8 cm thickness between them. Figure 3 shows the lower section of the wooden box. The four-core cable characteristics and thermal resistivity of the soil are given in Table 1, which is used in the experimental study.

The construction of the distribution cable and thermocouple junction (K) installation position is shown in Fig. 4. In this figure, three thermocouples are used to measure the temperature of the cable layers and the surrounding soil. These thermocouples are

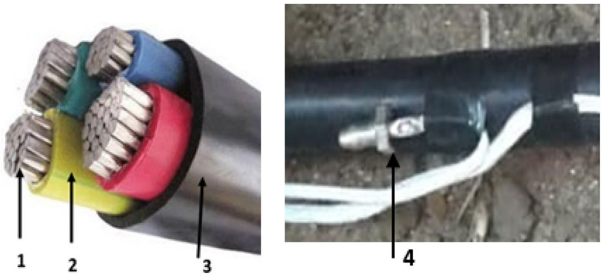

Fig. 4 Construction of the proposed cable: 1-aluminum conductor, 2-XLPE insulation, 3-PVC outer sheath, and 4-Thermocouple installation

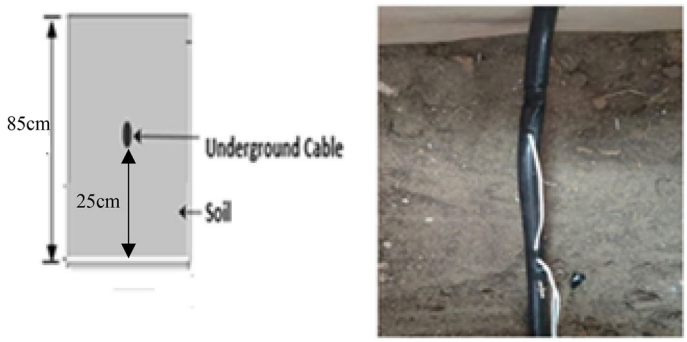

Fig. 5 Schematic design of laying cable direct in soil

placed in direct contact with the XLPE insulation, the outer PVC sheath of the cable, and in the soil around the cable.

The parameters of the soil used in the directly buried method are a mixture of 15% clay, 85% sand and 0.03 percent humidity content of the soil (m^3/m^3). The wet thermal resistivity of the soil is 0.968 (°Cm/W), and the dry density is 1588 (Kg/m^3) [26] at the surrounding temperature (θ_a) of 25 °C. As given in Fig. 5, three thermocouples are installed in different places to monitor the temperature of the cable parts and their surrounding soil. These thermocouples give an output in mV, which represents the temperature in the system.

The cable is installed inside the PVC duct with a diameter of 3.81 cm and a wall thickness of 2 mm and buried in the same soil illustrated above. The duct hole was closed on both sides using thermal insulation as shown in Fig. 6. The laboratory experiments on testing cable were carried out during one season of the year. Moreover, the temperature of the surrounding medium inside the laboratory is constant and not affected by external weather factors. To ensure the stability of the soil properties, the time difference between each installation method is one month.

Transient thermal modeling of underground distribution cables

Transient thermal model of cable installed direct in the soil

The cable layers are performed by lumped circuit thermoelectric equivalent method (TEE) according to IEC 60,853-2 [27–31, 30, 31]. As shown in Fig. 7a, the thermal analysis at each node of the thermal model of distribution cable directly buried in the soil.

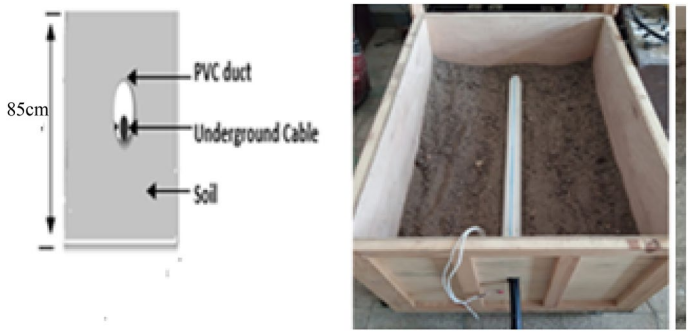

Fig. 6 Schematic design of laying cable in PVC duct

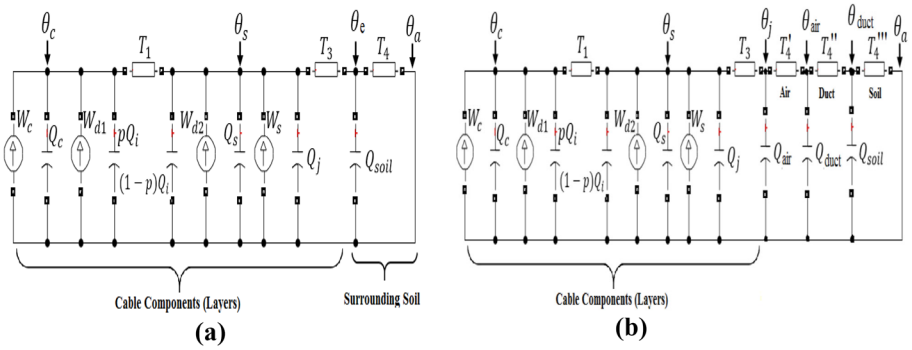

Fig. 7 Thermal equivalent circuit for single core cable parts and the around soil, **a** for direct buried, **b** for cable install in duct and buried in the soil

The thermal circuit contains on three thermal capacitances. Q_1, Q_3, and Q_4 are calculated by using IEC 60,853-2 [27]:

$$Q_1 = Q_c + \rho.Q_i \tag{1}$$

$$Q_3 = (1-\rho).Q_i + Q_s + Q_j \tag{2}$$

$$Q_4 = Q_{\text{soil}} \tag{3}$$

where Q_{soil},Q_s,Q_j,Q_i and Q_c are the thermal capacitances of surrounding soil, screen, jacket, insulation and conductor, respectively.T_4, T_1 and T_3 are the thermal resistances of surrounding soil, insulation and jacket, respectively. The thermal resistances of the metallic layers are ignored.θ_e, θ_s and θ_c are the jacket, screen and conductor temperatures above the surrounding temperature (θ_a), respectively. Finally ρ is the coefficient of Van Wormer [27].The cable losses of the conductor (W_c) are produced by the resistance of the conductor. Screen losses (W_s) are due to circulating current flowing in the cable sheath. The insulation losses (W_{d1}) and (W_{d2}) are dependent on the insulation material type and ignored for low-voltage cables. The different losses of the cable component are calculated according to IEC 60,287-1-3 [1].

$$W_c = I^2.R_{ac} \tag{4}$$

$$W_s = W_c.\lambda_1 \tag{5}$$

$$W_d = 2\pi.f.C.V_o^2.\tan(\sigma) \tag{6}$$

where I, R_{ac} and λ_1 are load current, conductor electrical resistance and sheath loss factor, respectively. V_o, f, C and tan (σ) are the phase voltage, system frequency (Hz), the electrical capacitance and the insulation loss factor, respectively. The thermal capacitances and resistances of the cable in each part and the around soil are calculated as given in [1, 27].

$$Q_c = C_{pc}.A_c \tag{7}$$

$$Q_i = \frac{\pi}{4}\left(D_i^2 - d_c^2\right)C_{pi} \tag{8}$$

$$Q_s = \frac{\pi}{4}\left(D_s^2 - D_i^2\right)C_{ps} \tag{9}$$

$$Q_j = \frac{\pi}{4}\left(D_e^2 - D_s^2\right)C_{pj} \tag{10}$$

$$Q_{\text{soil}} = \pi\left(L^2 - \left(\frac{D_e}{2}\right)^2\right)C_{\text{psoil}} \tag{11}$$

$$T_1 = \frac{\rho_i}{2\pi}\ln\left(\frac{D_i}{d_c}\right) \tag{12}$$

$$T_3 = \frac{\rho_j}{2\pi}\ln\left(\frac{D_e}{D_s}\right) \tag{13}$$

$$T_4 = \frac{\rho_{\text{soil}}}{2\pi}\left\{\ln\left(\frac{4L}{D_e}\right) + \ln\left(1 + \left(\frac{2L}{S}\right)^2\right)\right\} \tag{14}$$

where d_c, D_i, D_s and D_e are the external diameter of the conductor, insulation, screen and the cable surface, respectively. ρ_i, ρ_j and ρ_{soil} are the thermal resistivity of the cable different parts and soil around the cable. C_{pc}, C_{pi}, C_{ps}, C_{pj} and C_{psoil} are volumetric specific heat of each cable elements material and its surrounding soil. L, S and A_c are burial depth, the distance between conductor axes of the cables in case of flat formation and the area of the conductor, respectively. The current sources in the thermal model represent the heat sources in the metallic elements inside the cable.

Transient thermal model of cable installed inside PVC duct

To study the cable installed in the PVC duct, the different components such as the air and the duct medium are added to the thermal circuit as given in Fig. 7b. The thermal analysis at each node is represented in the following equations.

$$\theta_c' = \frac{1}{Q_1}.\left(W_c + W_{d1} - \frac{\theta_c - \theta_s}{T_1}\right) \tag{15}$$

$$\theta_s' = \frac{1}{Q_3}.\left(W_s + W_{d2} + \frac{\theta_c - \theta_s}{T_1} - \frac{\theta_s - \theta_e}{T_3}\right) \tag{16}$$

$$\theta_j' = \frac{1}{Q_{\text{air}}}.\left(\frac{\theta_s - \theta_j}{T_3} - \frac{\theta_j - \theta_{\text{air}}}{T_4'}\right) \tag{17}$$

$$\theta_{\text{air}}' = \frac{1}{Q_{\text{duct}}}.\left(\frac{\theta_j - \theta_{\text{air}}}{T_4'} - \frac{\theta_{\text{air}} - \theta_{\text{duct}}}{T_4''}\right) \tag{18}$$

$$\theta_{\text{duct}}' = \frac{1}{Q_4}.\left(\frac{\theta_s - \theta_j}{T_4''} - \frac{\theta_j - \theta_{\text{air}}}{T_4'''}\right) \tag{19}$$

where Q_{air} and Q_{duct} are the thermal capacitances of air in the space between duct inner surface and outer surface of cable jacket and the cable duct, respectively. T_4' is the air thermal resistance between the inner surface of the duct and the cable jacket. The thermal resistance of the soil around the duct is defined as T_4'''. T_4'' indicates to the duct thermal resistance. The thermal resistances of the metallic layers are ignored.θ_{duct} and θ_{air} are the duct and air temperatures °C above surrounding temperature, respectively. The additional thermal capacitances and resistances of cable in each part and the around soil are calculated as given in [1, 28].

$$Q_{\text{air}} = \frac{\pi}{4}\left(D_{di}^2 - D_e^2\right) C_{\text{pair}} \tag{20}$$

$$Q_{\text{duct}} = \frac{\pi}{4}\left(D_{\text{do}}^2 - D_{\text{di}}^2\right) C_{\text{pduct}} \tag{21}$$

$$\rho = \frac{1}{2\ln\left(\frac{D_i}{d_c}\right)} - \frac{1}{\left(\frac{D_i}{d_c}\right)^2 - 1} \tag{22}$$

$$T_4 = T_4' + T_4'' + T_4''' \tag{23}$$

$$T_4' = \frac{U}{1 + 0.1(V + Y\theta_{\text{duct}})D_e} \tag{24}$$

$$T_4'' = \frac{\rho_d}{2\pi}\ln\left(\frac{D_{\text{do}}}{D_{\text{di}}}\right) \tag{25}$$

$$T_4''' = \frac{\rho_{\text{soil}}}{2\pi}\left\{\ln\left(\frac{4L}{D_{do}}\right) + \ln\left(1 + \left(\frac{2L}{S}\right)^2\right)\right\} \tag{26}$$

where D_{do} and D_{di} are the PVC duct and inner PVC duct, respectively · The thermal resistivity of the PVC duct is defined asρ_d. The V, Y and U are constants according to IEC 60,287 [1] in case of the cables installed in duct and buried in the soil.C_{pduct} and C_{pair} are the volumetric specific heat of duct and air inside the duct.

The effect of harmonic distortion on the distribution cable losses

In this study, four-core cables with and without harmonic current effects are investigated. The fundamental frequency and harmonic order frequencies are considered in transient harmonic analysis. Taking into account harmonic current at each frequency, total harmonic distortion current losses are estimated. Odd orders of harmonic current are determined. The conductor resistance (Ω/m) without harmonic effects according to IEC-60287-1 is illustrated as follows [1].

$$R_{ac} = R_{dc}\left(1 + Y_s + Y_p\right) \tag{27}$$

$$Y_s = \frac{x_s^4}{192 + 0.8x_s^4} \tag{28}$$

$$Y_p = \left[\frac{x_p^4}{192 + 0.8x_p^4}\right].\left(\frac{d_c}{S}\right)^2.\left[0.312.\left(\frac{d_c}{S}\right)^2\left(\frac{1.18}{\frac{x_p^4}{192+0.8x_p^4} + 0.27}\right)\right] \tag{29}$$

where R_{dc} denotes the resistance of the DC conductor at maximum operating temperature (θ). Y_p and Y_s are the proximity and skin effect factors can be used to calculate the effects of harmonic current orders on the increase of temperature in distribution cable layers. x_p and x_s equations are given in [1].

Due to increasing harmonic current orders, this will cause an increase in the $\mathrm{R_{ac}}$ as a consequence dependent on proximity and skin factors. These factors are dependent on frequency change as follows [1, 29].

$$x = 0.01528\sqrt{\frac{f.\mu}{R_{dc}}} \tag{30}$$

$$Y_s = 10^{-3}\begin{pmatrix} -1.04x^5 + 8.24x^4 \\ -3.24x^3 + 1.447x^2 \\ -0.2764x + 0.0166 \end{pmatrix}, if\ x \le 2 \tag{31}$$

$$Y_s = 10^{-3}\begin{pmatrix} -0.2x^5 + 6.616x^4 \\ -83.343x^3 + 500x^2 \\ -1061.9x + 769.63 \end{pmatrix}, if\ 2 < x \le 100 \tag{32}$$

$$Y_p = Y_s.\left(\frac{d_c}{S}\right)^2.\left(\frac{1.18}{Y_s + 0.27} + 0.312.\left(\frac{d_c}{S}\right)^2\right) \tag{33}$$

where x and μ are the skin parameters and magnetic permeability, respectively. Consequently, for a non-sinusoidal current as a result of harmonic orders, the I_{rms} is root-mean-square current can be defined in relation to harmonic order (*h)* as given in (34).

The losses in distribution cables depend not only on the total harmonic distortion (THD), but also on the magnitude of each harmonic order. In [4], IEEE Standard 519 recommends a limit on both of them. The THD is used to express the effect of harmonic currents on the distribution cable. It is a percentage, as shown in (35).

$$I_{rms} = \sqrt{I_1^2 + \sum_{h=2}^{\infty} I_h^2} = I_1 \sqrt{1 + (THD)^2} \tag{34}$$

$$THD = \frac{\sqrt{\sum_{h=2}^{\infty} I_h^2}}{I_1} \tag{35}$$

In the case of odd harmonic current orders, the conductor power loss W_c can be calculated at each frequency and summed by:

$$W_c = (I_1)^2 . \left(R_{ac(1)} + \sum_{h=3}^{\infty} H_h^2 . R_{ac(h)} \right) \tag{36}$$

where I_1, I_h and $R_{ac(1)}$ are the fundamental current component harmonic current and AC conductor resistance at fundamental frequency in case of non-sinusoidal waveform, respectively. H_h is the percentage harmonic load current. $R_{ac(h)}$ is the conductor resistance of harmonic frequency.

In this article, the current harmonic distortion for the distribution cable system is taken into account and all the odd order harmonic orders up to the 23rd are studied. All the higher orders, even zero harmonic orders, are neglected.

Results of the proposed study system

Load current cycle and harmonics data

The calculations are carried out when each phase of the tested cable is loaded by different linear and nonlinear loads, as seen in Table 2. The three phases of the cable are loaded with nonlinear loads such as compact fluorescent lamps, adjustable speed drives, auto-transformers, and power supplies.

The current of the connected loads at each phase is balanced but with a different percentage value of THD. The harmonic current orders in phase A are produced with total harmonic distortion (THD = 50.8%). It is read by fluke 125 as shown in Fig. 8.

Experimental results of the proposed system

The dynamic temperature obtained from experimental results included the effect of linear and nonlinear loads on the cable layers and their surrounding soil. Figure 9 illustrates the flowchart of the experimental dynamic temperature calculation. The study was done on one meter of four-core 380 V cable buried directly in the soil and also inside a PVC duct in the soil in an isolated wooden box. The two small cable sections outside that box are connected with source and load panels.

Table 2 Current and total harmonic distortion on each phase

Phase	Current (A)	Without harmonic loads		With harmonic loads		
		Loads types	THD %	Loads types	Source	THD %
A	18.22	Resistance banks	4.35	Fluorescent lamps	Single	50.8
				One branch of resistance bank	Single	
				Adjustable speed drive	Three	
B	18.78	Resistance banks	4.35	Auto-transformer	Single	34.4
				Two branches of resistance bank	Single	
				Adjustable speed drive	Three	
C	18.32	Resistance banks	4.35	Power supply	Single	44.8
				Tungsten coils	Single	
				Adjustable speed drive	Three	

The temperature of these sections outside the wooden box is lower than the cable inside the soil, approximately equal to the laboratory temperature, because the temperature of the surrounding medium inside the laboratory is not affected by external weather factors. The used soil is a mixture of 15% clay, 85% sand, and a 0.03 percent humidity content (m^3/m^3). The temperature of the cable layers and surrounding soil is measured by thermocouples connected with an amplifying and comparator circuit. The output of the thermocouples in mV is read every two hours and converted into an equivalent temperature in °C.

The comparison between the cable parts and the surrounding soil temperature is shown in Fig. 10a, which is installed by direct burring in the soil and loaded with linear loads such as resistive banks and tungsten coils. After 72 h, the maximum insulation temperature reached 65 °C and the maximum soil temperature was around 52 °C.

It is also observed that when the cable is loaded with nonlinear loads, the harmonic current orders on phase A produced with THD = 50.8% are read by fluke 125 as given in Fig. 8. This effects the temperature of cable parts and the surrounding soil. At the same loading time, the maximum insulation temperature was approximately 72 °C, and the maximum soil temperature was 56 °C. The results are obtained by applying THD = 50.8%, which causes an increase in the insulation temperature of distribution cable as compared with its value when loaded with linear loads at frequency (50 Hz).

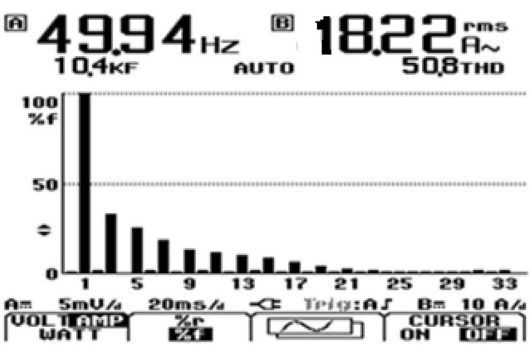

Fig. 8 Current harmonic orders by fluke 125

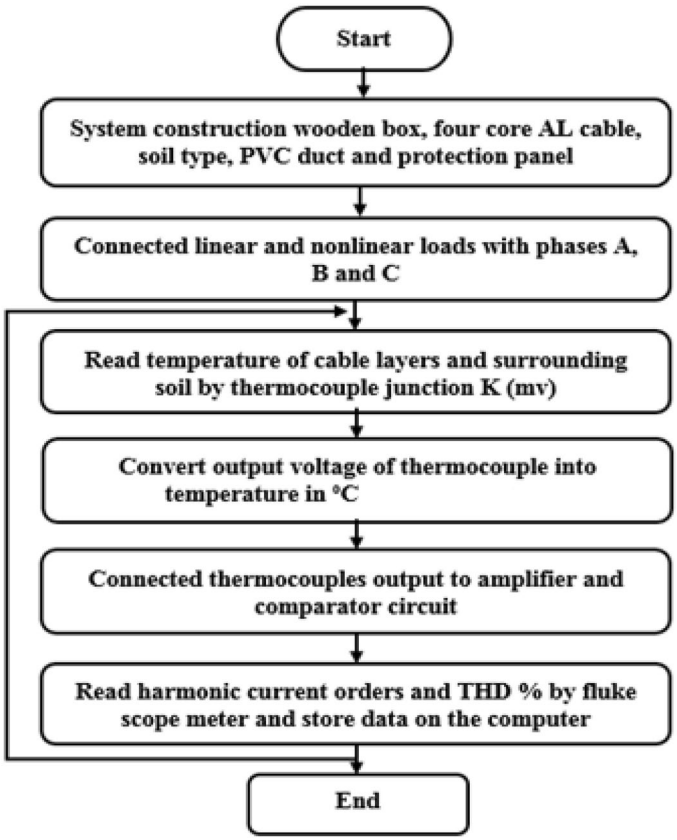

Fig. 9 Used flowchart

In the following study, the cable was installed in the PVC duct with a diameter of 3.81 cm and a wall thickness of 2 mm and buried in the same soil type. As shown in Fig. 10b, temperature readings differ in linear and nonlinear connected loads.

It is noticed when the cable is loaded with linear loads, the maximum insulation temperature increases to 70 °C after 72 h and the maximum soil temperature reaches about 33.5 °C.

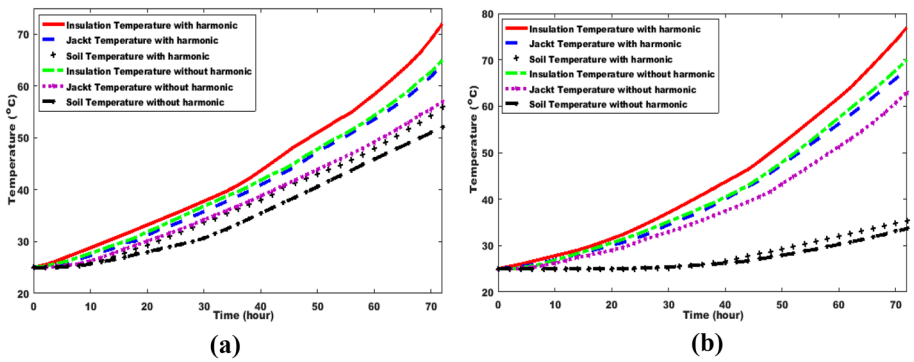

Fig. 10 Comparison of dynamic temperature obtained from experimental measurements **a** with linear and nonlinear loads at direct buried, **b** with linear and nonlinear loads at installed inside PVC duct in the soil

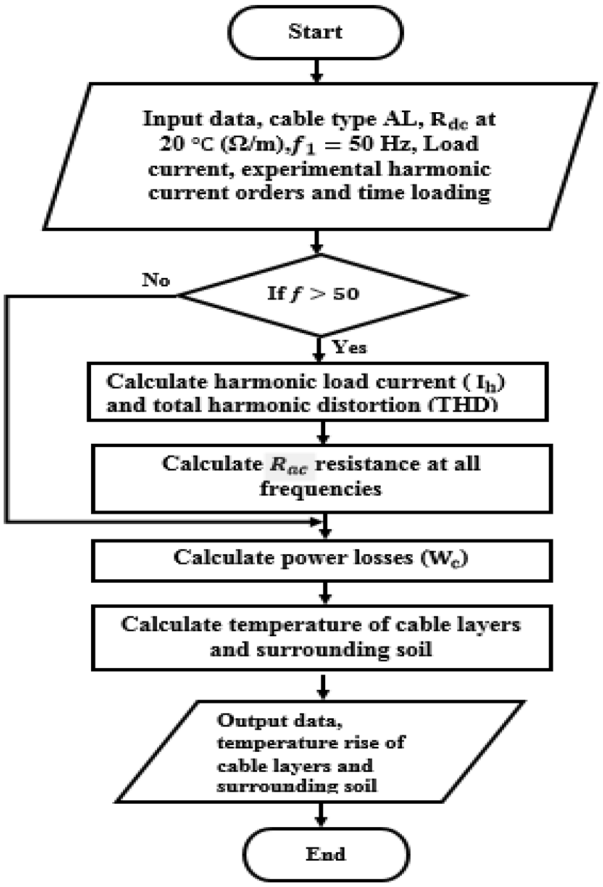

Fig. 11 Used flowchart of MATLAB program

But in the case of the cable being loaded with nonlinear loads at the same harmonic current orders with THD = 50.8%, the maximum insulation temperature increased to 77 °C and the maximum soil temperature was about 35.5 °C at the same loading time. The results are obtained by applying THD = 50.8%. When installed in PVC duct, the insulation temperature of the distribution cable rises to ∼ 10% as compared to its value in linear loads at frequency (50 Hz).

The reason for that increase in insulation temperature by 7 °C and the small change in the soil temperature is the thermal resistance of the PVC duct and air between the PVC duct inner surface and the outer surface of the cable jacket. The PVC duct prevents all the generated heat by the cable losses from reaching the surrounding soil.

The presence of harmonic current orders and installation in PVC duct have a significant impact on the temperature of the cable parts and the surrounding soil, according to one interesting observation.

Simulation results of thermal model

The thermal analysis of the distribution cable layers and the surrounding soil is solved using the MATLAB program. Figure 11 shows the flowchart of the MATLAB program. The temperature obtained from simulation results included the effect of

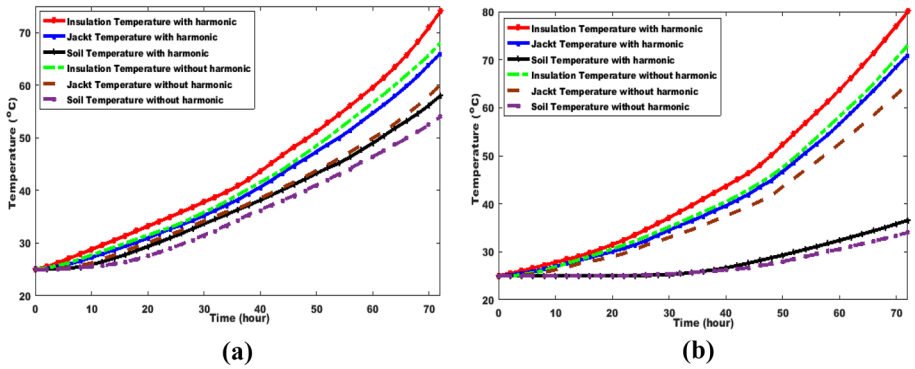

Fig. 12 Comparison of dynamic temperature of the cable layers and surrounding soil using thermal method **a** With sinusoidal and non-sinusoidal current at direct buried, **b** with sinusoidal and non-sinusoidal current source at installed inside PVC duct in the soil

sinusoidal and non-sinusoidal current waveforms on the cable layers and their surrounding soil. The soil used in the thermal analysis has the same properties as the one used in the experimental study. A study was carried out on the same four-core 380 V cable buried directly in the soil and also in a PVC duct buried in the soil. In the case of a cable that is directly buried in the ground, Fig. 12a depicts a comparison of temperature cable elements and the soil surrounding them.

When the cable is loaded with a sinusoidal current waveform at fundamental frequency (50 Hz), the maximum insulation temperature reaches about 68 °C after 72 h and the maximum soil temperature reaches 54 °C. A non-sinusoidal current waveform with a harmonic disturbance percentage of fundamental current THD = 50.8% as given in Fig. 8 noticed the effect of harmonic current orders on the temperature of the distribution cable. During the loading process, the insulation temperature rises to 74 °C, while the surrounding soil temperature rises to 58 °C.

The results were obtained by applying THD = 50.8%, which causes an increase in the insulation temperature of distribution cable by ∼ 8.8% as compared with its value in a sinusoidal current waveform at fundamental frequency (50 Hz). It was also observed in the case of the cable installed in a PVC duct and buried in the same soil type. That there was a greater increase in temperature when compared to the one that was buried directly. Fig. 12b shows the comparison between the temperatures of the cable elements and the soil around the cable in the two methods.

When the cable was loaded with a non-sinusoidal current waveform at fundamental frequency (50 Hz), the maximum insulation temperature increased to 73 °C and the maximum soil temperature reached about 34 °C after 72 h. It is also noticed that when the cable is loaded with non-sinusoidal current waveform at the same harmonic current orders with THD = 50.8%,the maximum insulation temperature increased to 80 °C and the maximum soil temperature reached about 36.5 °C at the same loading time. The results were obtained by using THD = 50.8%, which causes a ∼ 9.6% increase in distribution cable insulation temperature when compared to its value in sinusoidal current waveform.

Temperature maps of the cable layers and its surrounding medium using finite element method (FEM)

FEM is used to study the temperature of the underground distribution cable layers and the medium around them. This is simulated by using the (COMSOL) multiphysics program. Adiabatic boundaries are established on both the right and left sides of the installation, far away from the cables and the installation's bottom (i.e., heat flux equals zero). As a result of this set of boundary conditions, a negligible error in the calculation of transient temperature Furthermore, the heat generated in each cable layer is used as a source of heat for the model in two dimensions. The boundary conditions are depicted with heat flow considered in all directions. The FEM model is used to create the heat map of the temperature distribution in the cable and surrounding soil at constant thermal resistivity of the soil. The cable is loaded with a sinusoidal current waveform at a fundamental frequency of 50 Hz. Figure 13a shows the heat transfer of the cable components and their surrounding soil after 72 h of installation when the cable is directly buried in the soil. The insulation temperature is found to be ~ 65.4 °C.

A similar study was carried out on the cable when it was loaded with a non-sinusoidal current waveform at a fundamental frequency (50 Hz) for 72 h when the cable was installed directly buried in the soil. The insulation temperature rises to ~ 71 °C, rather than the 65.4 °C shown in Fig. 14a. However, if the cable is installed inside PVC duct, buried in the same soil type, and loaded with the same loads, the cable's insulation temperature is raised to ~ 80 °C rather than 72.7 °C as shown in Fig. 14b.

The results of the finite element method (FEM) are almost in agreement with the thermal calculation analysis and experimental measurement, with about 1.5 °C differences between the three calculations at the same conditions.

Comparison of the experimental and simulation results

Table 3 gives a summary of the experimental and simulation results obtained from the study of linear and nonlinear loads on the distribution cable. From the study and calculations performed, it is concluded that the type of installed methods of cable and connected load types affect the temperature of the insulation and the soil surrounding the

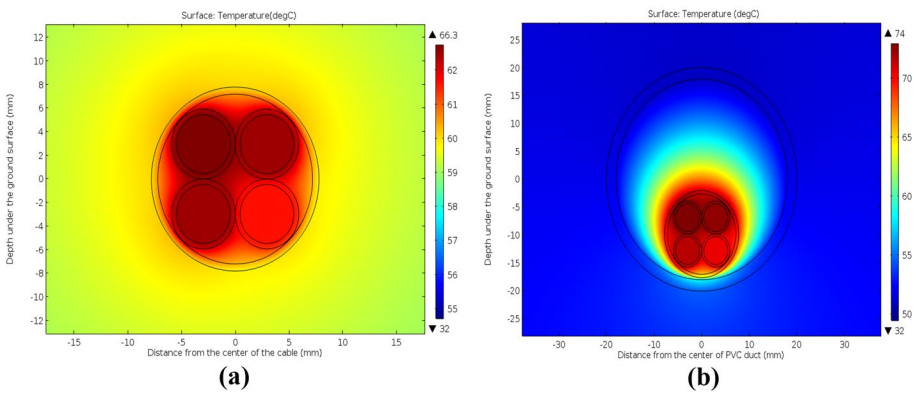

Fig. 13 COMSOL heat maps of cable layers and its surrounding medium of 380 kV without harmonic currents effect: **a** The cable directly buried in the soil. **b** The cable is installed inside PVC duct in the soil

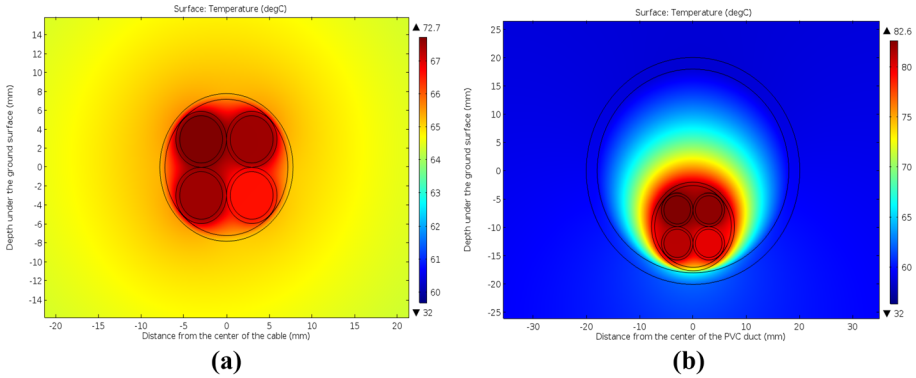

Fig. 14 COMSOL heat maps of cable layers and its surrounding medium of 380 kV with harmonic currents effect: **a** The cable directly buried in the soil. **b** The cable is installed inside PVC duct in the soil

Table 3 Summary of the obtained temperature from experimental and simulation results of tested cable

		Experimental results	Simulation results
Cable installed direct buried in the soil			
Maximum insulation temperature (°C)	Without harmonic	65	68
	With harmonic	72	74
Maximum jacket temperature (°C)	Without harmonic	57	60
	With harmonic	64	66
Maximum soil temperature (°C)	Without harmonic	52	54
	With harmonic	56	58
Cable installed in PVC duct and buried in the soil			
Maximum insulation temperature (°C)	Without harmonic	70	73
	With harmonic	77	80
Maximum jacket temperature (°C)	Without harmonic	63	65
	With harmonic	68	71
Maximum soil temperature (°C)	Without harmonic	33.5	34
	With harmonic	35.5	36.5

distribution cable. As shown in (35), percentage THD changes root-mean-square load current cycle values.

The experimental results were obtained by applying the same percentage of THD to the cable installed in a PVC duct, which caused an increase in the insulation temperature of the distribution cable by ∼ 6.9% as compared with its value when buried directly with nonlinear loads. Additionally, the soil temperature surrounding the cable decreases by ∼ 36.6% as compared with its value in direct burial.

Similar results have been obtained from simulation calculations and FEM by applying the same percentage THD to the cable installed in PVC duct, which caused an increase in the insulation temperature of the distribution cable by ∼ 8.1% as compared with its value when buried directly with a non-sinusoidal current waveform at fundamental frequency (50 Hz). Moreover, the soil temperature surrounding the cable has decreased to ∼ 37.1% as compared with its value in direct burial. The results of the MATLAB program are almost equivalent to the results obtained by the experimental results, with

a slight difference of about 3 °C between the two calculations at constant thermal soil resistivity. After the calculations had been performed, a noteworthy of attention is that the harmonic current orders were added to the cyclic load current. That harmonic current orders result in a THD percentage of 50.8% in two installation methods It has been found that in the case of direct burring, there is a serious rise in the temperature of the cable elements and the surrounding soil. But in PVC duct burring, there has not been a significant rise in the temperature of the surrounding soil.

Conclusions

In this article, the laboratory experimental study of an underground distribution low-voltage cable that is installed directly in the soil and inside a PVC duct in the soil is performed. The two installation methods are based on the IEC 60,287-1-3 and IEC 60,853-2 standards. The experimental test is carried out on a four-core 380 V cable to investigate the effect of harmonic current orders on the elements of the distribution cable. An increase in temperature has been observed in cable layers installed inside PVC duct. It is higher than in direct burring in the soil, in the presence of harmonic current orders. The insulation temperature rises between 7 and 8 °C depending on the percentage THD and duct installation method. Also, it is noted that there is a significant decrease in the temperature of the surrounding soil in the case of PVC duct installation. This is due to the thermal resistance of the PVC duct being high compared with the thermal resistance of the soil, which causes the retention of produced heat inside the PVC and the cable ampacity to decrease. It is concluded that the results have been obtained from simulation programs, whether MATLAB or (COMSOL) multiphysics programs, with a slight difference from the results of the experimental study.

Acknowledgements
Not applicable.

Author contributions
The authors confirm contribution to the paper as follows: WAAS conceived the experimental design of the study. TMZ Elsharkawy developed the model, analyzed the data, and wrote the manuscript with support from WAAS and GFAO. WAAS, GFAO, and TMZE contributed to the final version of the manuscript. All authors read and approved the final manuscript.

Funding
This research received no specific grant from any funding agency in the public, commercial, or not-for-profit sectors.

Availability of data and materials
The data that support the findings of this study are available on request from the corresponding author.

Declarations

Competing interests
The authors declare that they have no competing interests.

Received: 16 August 2022 Accepted: 25 September 2022
Published online: 10 October 2022

References

1. IEC publication 60287-1-3 (1992) Calculations of the continuous current rating of cables (100% load factor)
2. Kaushik A, Varanasi J (2014) Harmonic voltage distortions in power systems due to nonlinear loads. Int J Appl Power Eng 3(1):67–74
3. Testa A et al (2007) Interharmonics: theory and modeling. IEEE Trans Power Deliv 22(4):2335–2348
4. IEEE Std. 519-1992 (1992) IEEE recommended practices and requirements for harmonic control in electrical power systems

5. Ghijselen JA, Ryckaert WA, Melkebeek JA (2004) Influence of electric power distribution system design on harmonic propagation. Electr Eng 86:181–190
6. BS EN IEC, BS EN 61000-3-2 Ed.2:2001 IEC 61000-3-2 Ed.2:2000Electromagnetic compatibility (EMC), part 3–2: limits for harmonic current emissions (equipment input current up to and including 16 A per phase) (2001)
7. Al-Saud MS, El-Kady MA, Findlay RD (2008) Combined simulation experimental approach to power cable thermal loading assessment. IET Gener Transmiss Distrib 2(1):13–21
8. Gouda OE, Osman GF, Salem WA, Arafa SH (2018) Cyclic loading of underground cables including the variations of backfill soil thermal resistivity and specific heat with temperature variation. IEEE Trans Power Deliv 33(6):3122
9. Diaz-Aguilo M, Leon FD, Jazebi S, Terracciano M (2014) Ladder-type soil model for dynamic thermal rating of underground power cables. IEEE Power Energy Technol Syst J 1:21–30. https://doi.org/10.1109/jpets.2014.2365017
10. Salata F, Nardecchia F, de Lieto Vollaro A, Gugliermetti F (2015) Underground electric cables a correct evaluation of the soil thermal resistance. Appl Therm Eng 78:268–277. https://doi.org/10.1016/j.applthermaleng.2014.12.059
11. Rasoulpoor M, Mirzaie M, Mirimani S (2017) Thermal assessment of sheathed medium voltage power cables under non-sinusoidal current and daily load cycle. Appl Therm Eng 123:353–364. https://doi.org/10.1016/j.applthermaleng.2017.05.070
12. Shazly JH, Mostafa MA, Ibrahim DK, Zahab EEAE (2017) Thermal analysis of highvoltage cables with several types of insulation for different configurations in the presence of harmonics. IET Gener Transm Distrib 11(14):3439–3448. https://doi.org/10.1049/iet-gtd.2016.0862
13. Rerak M, Ocłoń P (2017) Thermal analysis of underground power cable system. J Therm Sci 26(5):465–471. https://doi.org/10.1007/s11630-017-0963-2
14. Salata F, Nardecchia F, Gugliermetti F, de Lieto Vollaro A (2016) How thermal conductivity of excavation materials affects the behavior of underground power cables. Appl Therm Eng 100:528–537. https://doi.org/10.1016/j.applthermaleng.2016.01.168
15. Rasoulpoor M, Mirzaie M, Mirimani SM (2017) Effects of non-sinusoidal current on current division, ampacity and magnetic field of parallel power cables. IET Sci Meas Technol 11(5):553–562. https://doi.org/10.1049/iet-smt.2016.0549
16. Cywiński A, Chwastek K (2019) Modeling of skin and proximity effects in multi-bundle cable lines, In: Progress in applied electrical engineering (PAEE), pp 1–5
17. Desmet J, Vanalme G, Belmans R, Van Dommelen D (2008) Simulation of losses in LV cables due to nonlinear loads, In: IEEE power electronics specialists conference, pp 785–790
18. Demoulias C, Labridis DP, Dokopoulos PS, Gouramanis K (2007) Ampacity of low-voltage power cables under nonsinusoidal currents. IEEE Trans Power Deliv 22:584–594
19. Yong J, Xu W (2016) A method to estimate the impact of harmonic and unbalanced currents on the ampacity of concentric neutral cables. IEEE Trans Power Del 31(5):1971–1979
20. Rice DE (1986) Adjustable speed drive and power rectifier harmonics their effect on power systems components. IEEE Trans Power Deliv 22:1–2
21. Sahin YG, Aras F (2007) Investigation of harmonic effects on underground power cables, In: Proc powereng, pp 589–594
22. BS EN, BS EN 50160:2000 (2000) Voltage characteristics of electricity supplied by public distribution systems
23. Al-Baldawi IA, Alsakini SR, Abed MS (2019) The effects of sand and pipes on the temperature distributions of the underground cable," ICSET
24. Bustamante S, Mínguezb R, Arroyoa A, Mananaa M, Lasoa A, Castroa P, Martineza R (2019) Thermal behaviour of medium-voltage underground cables under high-load operating conditions. Appl Therm Eng 156:444–452
25. Gouda OE, El Dein AZ (2021) Enhancement of the thermal analysis of harmonics impacts on low voltage underground power cables capacity," Elsevier, Applied Thermal Engineering, no 204
26. Gouda OE, Osman GFA, Salem WAA, Arafa SH (2018) Load cycling of underground distribution cables including thermal soil resistivity variation with soil temperature and moisture content. IET Gener Transm Distrib 12(18):4125–4133
27. IEC Standard 60853-2, "Calculation of the cyclic and emergency current ratings of cables. Part 2: cyclic rating factor of cables greater than 18/30 (36) kV and emergency ratings for cables of All voltages', 2088
28. Anders GA (2005) Rating of electric power cables in unfavorable thermal environment. IEEE Press Wiley-Interscience, Hoboken, NJ
29. Gouramanis K, Demoulias C, Labridis DP, Dokopoulos P (2009) Distribution of non-sinusoidal currents in parallel conductors used in three-phase four-wire networks. Electr Power Syst Res 79(5):766–780
30. Aras F, Bicen Y (2013) Thermal modelling and analysis of high-voltage insulated power cables under transient loads. Comput Appl Eng Educ 21:516–529
31. Stojanović M, Tasić D, Ristić A (2013) The influence of daily load profile on the heating of single-core XLPE cables buried in the ground. Autom Control Robot 12(3):157–167

Publisher's Note